ENCLOSURE 2

MFN 03-064

Response to NRC RAI numbers (187, 190, 191, 195, 202, 220, 225, 231, 232, 272, 296, 297, 327, 334–338, 345, 347, 349-359, 371-376, 378, and 379)

Q187. Page 2-5, Section 2.2.1.2 - For the last paragraph an elevation diagram would be helpful to the discussion.

R187. Please see Figure 187A and Figure 187B for details.

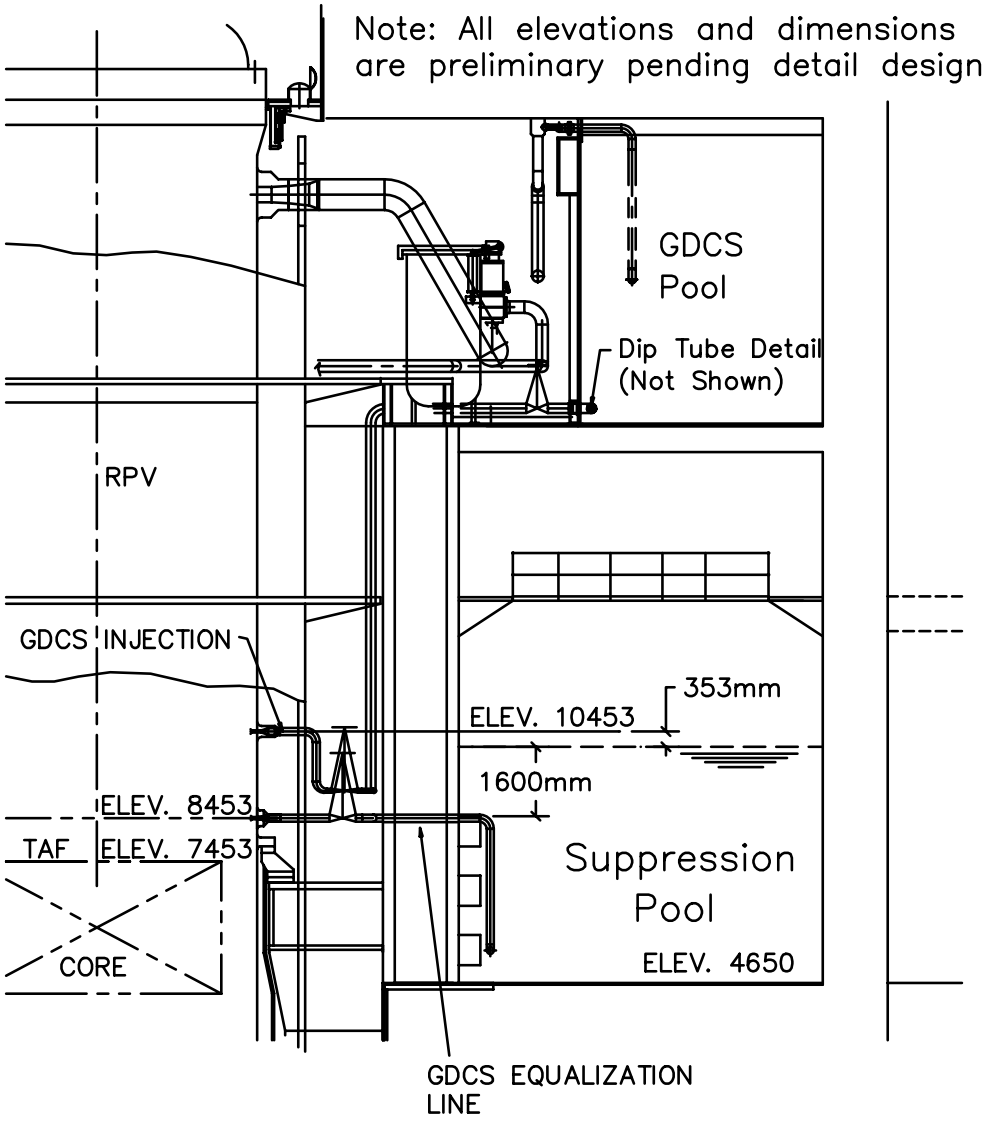

Figure 187A GDCS Equalization Line

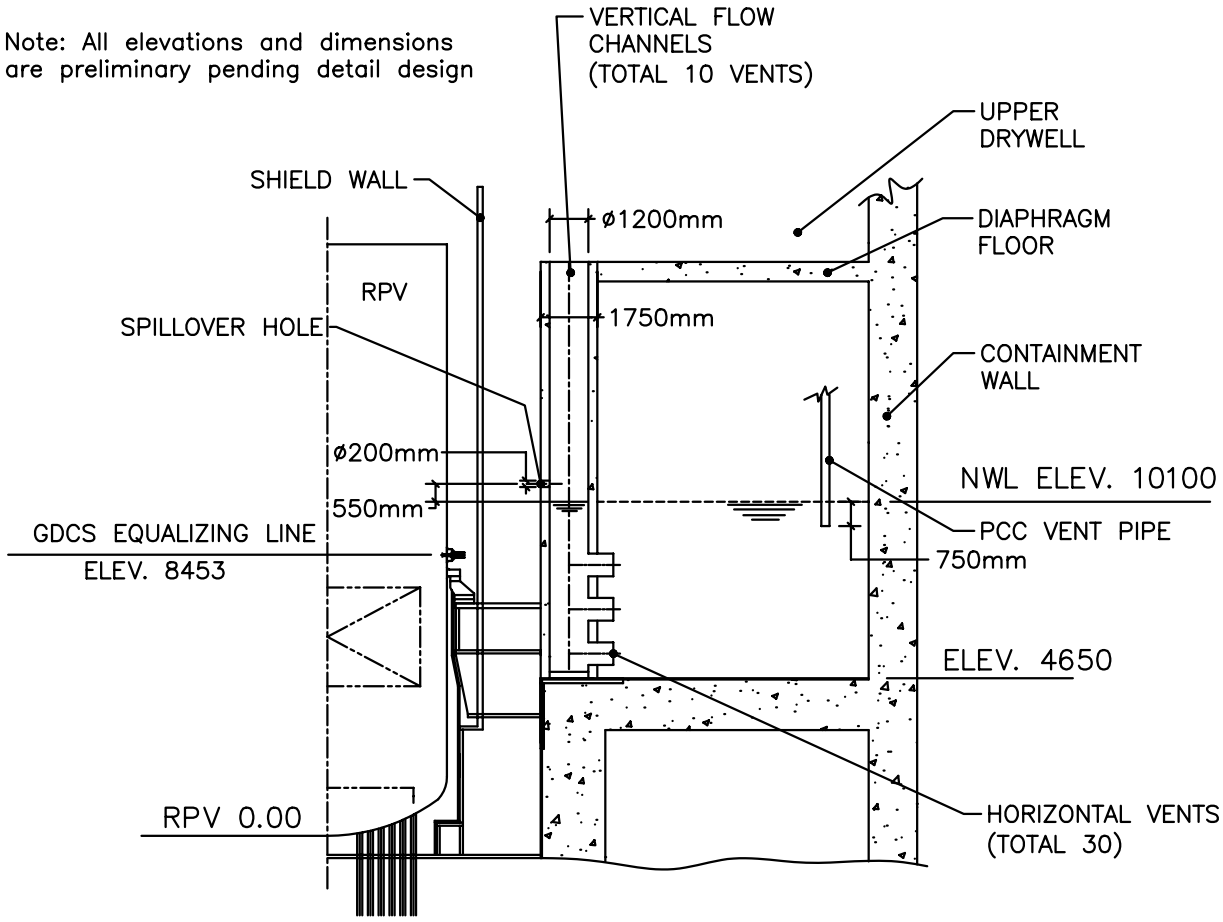

Figure 187B Spillover Hole Configuration

Q190. Page 2-9 (last paragraph) - It is stated that water collected in the drywell can spill into the wetwell through the spillover holes in the pipes connected to the horizontal vents. Please provide a sketch to show the elevation and diameter of the spillover holes and explain why their presence will not adversely affect horizontal vent clearing in a loss of coolant accident (LOCA).

R190. Please see Figure 187B (above) for details of the spillover holes. The holes lead from the annular region of the drywell (region surrounding the RPV) to the vertical vents, which lead to the horizontal vents under the water surface of the suppression pool. The spillover holes are 200 mm in diameter and are located about 550 mm above the normal level of the suppression pool water. One hole leads into each of the ten vertical vent pipes. The spillover holes provide a return path for water, which may accumulate in the lower drywell and the annular region of the drywell during a pipe break accident. The purpose of the spillover holes is to provide a means to limit the draw-down of the suppression pool water and thereby assure the PCCS heat exchanger vent submergence. Since the spillover holes are located above the normal water level in the vertical vents they have no impact upon the vent clearing process. The drywell atmosphere pressurizes the vertical vent water column and forces this level down to the first, second and sometimes even third horizontal vents in order to clear the vents and relieve the pressure differential.

Q191. Page 2-12 (4th paragraph) - Under what conditions will the subcooled water be sprayed into the steam dome of the reactor vessel? Where is the location of the source of the subcooled water?

R191. The subcooled water is sprayed into the steam through the feedwater spargers. The source is from the condensate/feedwater system. The assumption is that the feedwater system (e.g., motor driven pumps) are still available and operating.

Q195. Page 2-16 - (1) What is the water level in the loop seal (during normal full-power operation) between a passive containment cooling (PCC) unit and its condensate drain tank? (2) Is there any water in the PCC condensate drain tank during normal full-power operation?

R195. (1) The water level is provided as a loop seal, to prevent an open bypass from drywell to wetwell or vice versa. It's height is determined based on maximum long-term pressure differential postulated between the drywell and wetwell. The normal water level in the loop seal is approximately 2.5 m. To ensure the U-tube water seal on the condensate drain line section is full at all times, level detection instrumentation is provided to signal water level in this U-tube seal and, if a low-level condition is detected, makeup into the U-tube water seal is provided automatically via supply from the Condensate Storage and Transfer System. Level detection instrumentation is also present to detect a condition of water accumulation in the condensate drain tanks. If water level exceeds a pre-determined set-point level, drain valves are opened to drain this water into the drywell equipment drain sump.

(2) The drain tanks should not have any water in them during normal operation (other than minor condensation from moist drywell air). If water level did build up in the tank it would be drained as described in (1) above.

Q202. Page 3-27 (No.2 - B11/4) - It seems that the suction lines of the Reactor Water Cleanup/Shutdown Cooling (SDC) System are connected either to the RPV downcomer annulus or to the RPV bottom head and the injection lines are connected to the RPV via the main feedwater lines. (1) Please provide a sketch to show "inlet and outlet nozzles located diametrically across the downcomer." (2) There is a typographical error in the fourth column, "CFD code calculations show sort [sic] circuiting will not occur" should be replaced with CFD code calculations show short circuiting will not occur.

R202. Please refer to Figures 202A and 202B for details of the shutdown cooling suction nozzle and the feedwater nozzles.

The typographical error will be corrected in the report, NEDC-33079P "ESBWR Test and Analysis Program Description" and will specify:"CFD code calculations show short circuiting will not occur."

[[

]]

Figure 202A ESBWR RPV

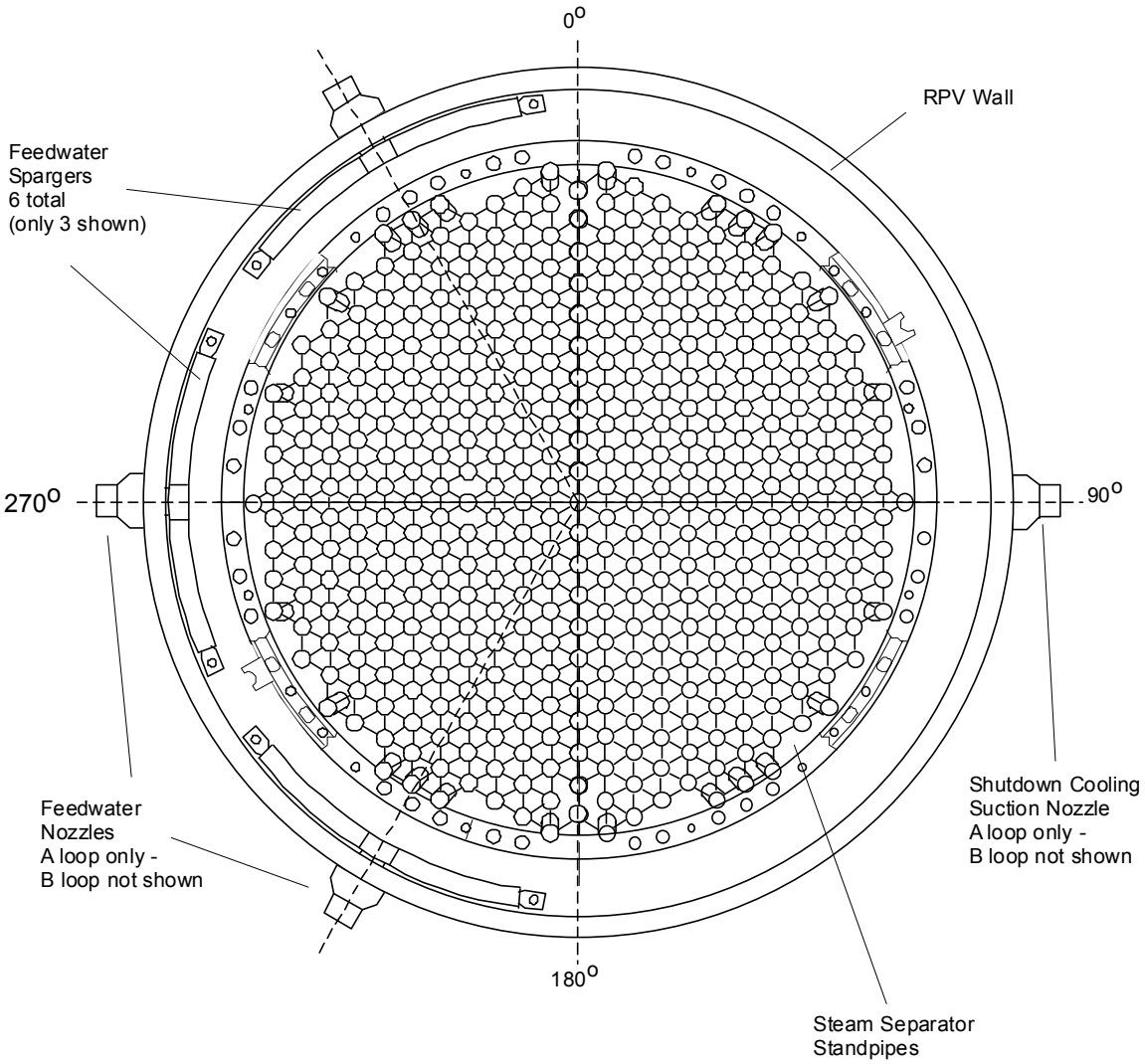

Name	Quantity	Elevation	Azimuth
Feedwater nozzles	6	18915 mm	30, 90, 150, 210, 270, 330
RWCU / Shutdown Cooling nozzles	2	17215 mm	90, 270

Note: All elevations and dimensions are preliminary pending detail design.

Section A-A

Figure 202B Section View A-A

Q220. Page 4-4, Section 4.1.2 - It is stated that "The high pressure makeup systems consist of the Isolation Condenser, which returns condensed steam to the vessel, and the Control Rod Drive System..." While the Isolation Condenser is a heat removal system, it seems inappropriate to call it a makeup system. Please correct this statement.

R220. The ICS is more of an inventory control system than a makeup system. It does not add inventory to the vessel from outside the containment but controls the loss of inventory. We will change the sentence to be more explicit as follows:

Transients end either by reaching a new steady state or by a scram, followed by inventory control using the Isolation Condenser System and the CRD System for high pressure makeup ~~The high pressure makeup systems consist of the Isolation Condenser, which returns condensed steam to the vessel, and the Control Rod Drive System, which can supply high pressure makeup~~ from the Condensate Storage Tank. System interactions including the effects of these systems have been considered in connection with LOCAs.

Q225. Page 5-13, Section 5.2 - Do the Moss Landing separator tests refer to the design to be used in ESBWR?

R225. [[

]]

Q231. Page A-41 (1st paragraph) - Please provide the basis for the hard seat equivalent flow area.

R231. [[

]]

Q232. Page A-42 (3rd paragraph) - Please provide a sketch to show the SLCS injection locations through the core shroud.

R232. The SLCS injects poison directly through the core shroud into the core bypass region. There are four azimuthal locations and four axial locations as shown in Figures 232.1 through 232.4. The dimensions and elevations as shown in the four figures are preliminary and may change during final design.

[[

]]

Q272. The report says that PANDA is "heavily instrumented with approximately 560 sensors" (page 5-7). However, it is not clear whether these 560 instruments are sufficient to provide a reliable (with built-in redundancy and cross-checking) mass and energy balance of steam, water, and noncondensible gases in the facility during a test that is consistent with the TRACG model nodalization of all components. Address the effectiveness of the instrumentation in providing a conclusive and detailed representation of these quantities.

R272. Instrumentation in the PANDA test facility provides measurements of important test parameters related to reactor safety evaluations, namely the DW and WW pressures and temperatures. The facility also underwent pretest characterization testing prior to the two major testing series (M-series and P-series) to determine irreversible line losses and system heat losses. Instrument diagrams (Figures 272.1 and 272.2) showing instrument locations in the PANDA facility vessels and the IC (typical of the PCCs also) are attached. Superimposed on these diagrams are the TRACG nodalizations for the corresponding components. It can be seen that the instrumentation does provide coverage of the important quantities calculated by the code. While no test facility, particularly an integral systems test facility as complex as PANDA, will ever have enough instrumentation to determine all details of its behavior, PANDA does have sufficient instrumentation to meet its experimental objectives, namely to demonstrate the behavior and operation of the passive cooling systems during the long-term cooling phase of the ESBWR LOCA transient and to provide a qualification basis for TRACG.

[[

]]

Figure 272.1. GDCS, DW, WW (SC) and SP Instrumentation Superimposed on TRACG Nodalization

[[

]]

Figure 272.2. IC/PCC Instrumentation Superimposed on TRACG Nodalization

Q296. Page 2-1, Section 2.2 - In ESBWR Test and Analysis Program Description, (NEDC-33079P) it is stated that the main vents will not open following the blowdown phase. In the PANDA tests, however, the main vents open on a number of occasions. It would be helpful to provide a section that describes the intended typicality and conservatisms in each of the tests and the particular aspects that dominate the results in terms of causing the main vents to open when they do.

R296. The main vents open for varying time periods during all of the PANDA tests except Test P6, where the IC was in operation. This behavior is shown by the main vent phase indicators in Figures 19a and b and the thermocouples near the WW end of the main vents (e.g., MTG.MV.1.4) in Figures 20a and b of the test reports. [[

]] The WW pressure increase is mainly the result of transfer of residual DW air with only a small contribution from the increase in WW steam partial pressure. [[

]]

Q297. Page 2-4, Section 2.3.5 - It is stated that "To cover this possibility in Test P6, the IC was valved out of service after seven hours of operation." Why was this time chosen? It would seem that a value closer to one hour would be more appropriate to cover this eventuality.

R297. [[

]] One of the major objectives of the test was to demonstrate the ability of the PCCs to assume the increased heat load after a long period of operation at a reduced load level.

Q327. It is assumed that the MSLB never occurs outside containment inside the outboard main steam isolation valve. Please explain why.

R327. The issue of pipe breaks between the MSIV and the containment boundary has been addressed previously for BWR's and the resolution has been accepted by the NRC. This issue is addressed in the Safety Analysis Report. The simple answer is that no pipe breaks or cracks are postulated in portions of piping from containment wall to and including the inboard or outboard isolation valves. The piping from the inboard isolation valve out to the outboard isolation valve is what we call "holy pipe". It is designed to very stringent requirements as dictated by the ASME code and as stipulated in the SAR. This piping must have somewhat low stress levels and fatigue usage. Welded attachments are avoided and welds are minimized. The isolation valves are located "as close as practical to the containment wall".

Please see the attached three pages from the ABWR Standard Safety Analysis Report for further details. Similar positions exist for all the operating BWR's licensed by the NRC. Since there is nothing fundamentally different in the ESBWR, the same approach applies to the ESBWR.

and valve bodies are also exempted from consideration of pipe break because of their greater wall thickness.

3.6.2.1.4 Locations of Postulated Pipe Breaks

Postulated pipe break locations are selected as follows:

3.6.2.1.4.1 Piping Meeting Separation Requirements

Based on the HELSA evaluation described in Subsection 3.6.1.3.2.2, the high-energy lines which meet the spatial separation requirements are generally not identified with particular break points. Breaks are postulated at all possible points in such high-energy piping systems. However, in some systems break points are particularly specified per the following subsections if special protection devices such as barriers or restraints are provided.

3.6.2.1.4.2 Piping in Containment Penetration Areas

No pipe breaks or cracks are postulated in those portions of piping from containment wall to and including the inboard or outboard isolation valves which meet the following requirement in addition to the requirement of ASME Code Section III, Subarticle NE-1120:

(1) The following design stress and fatigue limits of (a) through (e) are not exceeded. When meeting the limits of (a) and (d), earthquake loads are excluded (Subsection 3.6.1.1.1).

For ASME Code Section III, Class 1 Piping

(a) The maximum stress range between any two loads sets (including the zero load set) does not exceed 2.4 S_m, and is calculated* by Eq. (10) in NB-3653, ASME Code, Section III.

If the calculated maximum stress range of Eq. (10) exceeds 2.4 S_m, the stress ranges calculated by both Eq. (12) and Eq. (13) in Paragraph NB-3653 meet the limit of 2.4 S_m.

(b) The cumulative usage factor is less than 0.1.

(c) The maximum stress, as calculated by Eq. (9) in NB-3652 under the loadings resulting from a postulated piping failure beyond these portions of piping does not exceed the lesser of 2.25 S_m and 1.8 S_y except that, following a failure outside the containment, the pipe

* For those loads and conditions in which Level A and Level B stress limits have been specified in the Design Specification.

between the outboard isolation valve and the first restraint may be permitted higher stresses, provided that a plastic hinge is not formed and operability of the valves with such stresses is assured in accordance with the requirement specified in Subsection 3.9.3. Primary loads include those which are deflection limited by whip restraints.

For ASME Code Section III, Class 2 Piping

(d) The maximum stress, as calculated by the sum of Equations (9) and (10) in Paragraph NC-3653, ASME Code Section III, considering those loads and conditions thereof for which Level A and Level B stress limits are specified in the system's Design Specification (i.e., sustained loads, occasional loads, and thermal expansion) excluding an earthquake event does not exceed $0.8(1.8\ S_h + S_A)$. The S_h and S_A are allowable stresses at maximum (hot) temperature and allowable stress range for thermal expansion, respectively, as defined in Article NC-3600 of ASME Code Section III.

(e) The maximum stress, as calculated by Eq. (9) in NC-3653, under the loadings resulting from a postulated piping failure of fluid system piping beyond these portions of piping does not exceed the lesser of $2.25\ S_h$ and $1.8\ S_y$.

Primary loads include those which are deflection limited by whip restraints. The exceptions permitted in (c) above may also be applied provided that, when the piping between the outboard isolation valve and the restraint is constructed in accordance with the Power Piping Code ANSI B31.1, the piping is either of seamless construction with full radiography of all circumferential welds, or all longitudinal and circumferential welds are fully radiographed.

(2) Welded attachments, for pipe supports or other purposes, to these portions of piping are avoided except where detailed stress analyses, or tests, are performed to demonstrate compliance with the limits of Item (1).

(3) The number of circumferential and longitudinal piping welds and branch connections are minimized. Where penetration sleeves are used, the enclosed portion of fluid system piping is seamless construction and without circumferential welds unless specific access provisions are made to permit inservice volumetric examination of longitudinal and circumferential welds.

(4) The length of these portions of piping is reduced to the minimum length practical.

(5) The design of pipe anchors or restraints (e.g., connections to containment penetrations and pipe whip restraints) does not require welding directly to the outer surface of the piping (e.g., flued integrally forged pipe fittings may be used), except where such welds are 100% volumetrically examinable in service and a detailed stress analysis is performed to demonstrate compliance with the limits of Item (1).

(6) Sleeves provided for those portions of piping in the containment penetration areas are constructed in accordance with the rules of Class MC, Subsection NE of ASME Code Section III, where the sleeve is part of the containment boundary. In addition, the entire sleeve assembly is designed to meet the following requirements and tests:

(a) The design pressure and temperature are not less than the maximum operating pressure and temperature of the enclosed pipe under normal plant conditions.

(b) The Level C stress limits in NE-3220, ASME Code Section III, are not exceeded under the loadings associated with containment design pressure and temperature in combination with the safe shutdown earthquake.

(c) The assemblies are subjected to a single pressure test at a pressure not less than its design pressure.

(d) The assemblies do not prevent the access required to conduct the inservice examination specified in Item (7).

(7) A 100% volumetric inservice examination of all pipe welds would be conducted during each inspection interval as defined in IWA-2400, ASME Code Section XI.

See COL license information requirements in Subsection 3.6.5.3.

3.6.2.1.4.3 ASME Code Section III Class 1 Piping in Areas Other Than Containment Penetration

With the exception of those portions of piping identified in Subsection 3.6.2.1.4.2, breaks in ASME Code Section III Class 1 Piping are postulated at the locations identified in (1), (2), and (3) in each piping and branch run. Earthquake loads are excluded from (2).

(1) At terminal ends*.

(2) At intermediate locations where the maximum stress range as calculated by Eq. (10) exceeds 2.4 Sm, and

Q334. In the PANDA M-series and P-Series test reports, it is stated that with few exceptions the tests began at about one hour after the reactor scram. For some tests the initial core power was either below (e.g., Test P3) or above (Tests P2 and M7) the equivalent decay power at one hour after the reactor scram as discussed below.

Based on the SBWR decay heat power at one hour after the scram, the equivalent PANDA core power is 1.06 megawatts (MW) (or 1.056 MW as reported on page 22 of ALPHA-606, "PANDA Facility, Test Program and Data Base General Description"). Therefore, the initial core power of a PANDA M-series test should be set at about 1.06 MW if the test is to begin equivalently at one hour after the SBWR scram.

Based on the ESBWR decay heat power at one hour after the scram, the equivalent PANDA core power is 1.07 MW. This is calculated below with a PANDA scaling factor of [[ ]] and a decay heat power at [[ ]] of the full power (based on an ORIGEN calculation for a 10-by-10 boiling water reactor (BWR) fuel bundle at [[ ]]).

[[ ]]= 1.07 MW (or = 1.19 MW if using [[ ]] as the scale for PANDA)

Therefore, the initial core power of a PANDA P-series test for ESBWR should be at 1.07 MW (as a minimum) if the test is to begin equivalently at one hour after the scram. Note that PANDA M-series tests for the SBWR and P-series tests for the ESBWR have practically the same core power (namely, 1.07 MW vs. 1.06 MW), if the scale of PANDA is proved to be [[ ]] of the ESBWR.

Please describe how the core power was calculated and provide a table to list the initial core power and its equivalent time after the reactor scram for all PANDA M-series and P-series tests. If additional power was added to offset heat loss (or some power was subtracted for other reason), a statement should be made to this effect. Please list other initial test conditions in the same table (e.g., similar to the GIRAFFE table on p. 2-106 of NEDC-32606P, "SBWR Testing Summary Report").

R334. The RPV power for the PANDA M-series and P-series tests was calculated from a design specification that is based on the ANSI/ANS-5.1 standard. According to this specification, the shutdown power at one hour from the time of scram is 1.32% of the rated power. The RPV power for the M-series tests was calculated using a rated power of 2000 MW and a [[ ]] This gives an initial (one-hour) power of 1.06 MW. A time-dependent factor was applied to account for the release of stored energy from the RPV structure. This factor [[ ]] and reduced monotonically to 1.0 as the transient proceeded. Thus, the initial RPV heater power for the base-case M-series tests was [[ ]]

The power vs. time for all the M-series tests with the exception of M7 and M9 is given in Table 5.7-8 of Reference 1. The power vs. time for Test M9, which was initiated at an earlier time in the LOCA transient, is given in Table 5.7-9. The initial heater power for Test M9 was set at 1.4 MW, which was the upper limit of the PANDA heater capacity. To compensate for the fact that 1.4 MW is somewhat less than the scaled power at the at the time in the LOCA transient simulated by Test M9, the power was decreased more slowly than the corresponding decay power during the initial portion of the transient. Test M7 was run with a constant power of 1.13 MW. Detailed listings of the thermodynamic initial conditions for the M-series tests are given in Tables 5.7-11 through 5.7-19 of Reference 1.

The P-series tests were originally scaled to a 3600 MW ESBWR with a [[ ]] This gave a one-hour PANDA power of 1.19 MW. With the same [[ ]] applied for RPV structure stored energy, the initial heater power is [[ ]] When the ESBWR power was raised to 4000 MW, the PANDA P-series tests were recharacterized as [[ ]] with the RPV heater power maintained at an initial [[ ]] The variation of heater power with time for each of the P-series tests is shown in the figures labeled Figure Pn-2 (n = test number) in Reference 2. For all tests except P2, the variation of the heater power with time (i.e., ratio of instantaneous power to initial power) was the same for the P-series tests as for the M-series tests. The power vs. time for Test P2 is shown in Table 334.1. Detailed listings of the thermodynamic initial conditions for the P-series tests are given in Tables 2-3 through 2-9 of Reference 2.

Table 334.1
PANDA Heater Power for Test P2

Time from Scram (s)	Heater Power (MW)
1200 (Test Start)	1.4000
2250	1.4000
2500	1.3549
2940	1.2758
3600	1.2758
3650	1.2646
4000	1.2216
5000	1.1370
6000	1.0604
7000	1.0061
7200	0.9955
8000	0.9627
9000	0.9302
10000	0.9000
12000	0.8717
14400	0.8524

18000	0.8055
20000	0.7837
28800	0.7170

References

1. "TRACG Qualification for SBWR", NEDC-32725P, August 2002.

2. "TRACG Qualification for ESBWR, NEDC-33080P, August 2002.

3. "ESBWR Test Report", NEDC-33081P, August 2002.

4. "GIRAFFE SBWR Helium Series Test Report", NEDC-32608P, June 1996.

Q335. It appears that the initial passive containment cooling system (PCCS) vent submergence was set at [[ ]] for PANDA M-series tests, [[ ]] for PANDA P-series tests, and [[ ]] for GIRAFFE/Helium tests and System Interaction tests.

Q335.1. Please explain the basis for selecting this range of PCCS vent submergence [[ ]] in these tests.

R335.1. [[

]] In summary, the range of vent submergences in the three test programs had very little effect on the containment pressure and temperature and is judged not to be significant.

Q335.2. Was there any difference in the PCCS vent submergence before and after a test? If so, what was the difference?

R335.2. The increase in PCC vent submergence during the tests was negligible except for PANDA Tests M7 and P3, where it increased by about 0.04 m (Figure 336.2).

Q336.

Q336.1. Please provide a comparison of the important parameters including reactor pressure vessel (RPV), drywell (DW), and wetwell (WW) pressures, suppression pool (SP) level, and PCCS heat removal between PANDA M-series tests and PANDA P-series counterpart tests such as Test M7 vs. Test P3, and Tests M6/8 vs. Test P6.

R336.1. The pressures, suppression pool levels and PCC inlet flow rates for Tests M7 and P3 are compared in Figures 336.1 to 336.3. Similar comparisons for Tests M6/8 and P6 are shown in Figures 336.4 to 336.6.

[[

]]

In summary, the differences between Tests M7 and P3 and between Tests M6/8 and P6 can be explained in terms of differences in the initial and boundary conditions. All four tests show satisfactory PCCS response under a demanding set of conditions.

Q336.2. Provide a comparison of the important vessel and containment parameters (such as RPV water level, pressures of RPV and DW and WW, SP level, and GDCS pool level) of the three integral counterpart tests (GIRAFFE/Helium H1, PANDA M3, and either PANDA P1 or P4 (for t < 4 hours, without air injection to DW)). This question replaces a previous question (RAI 180). The counterpart tests were not specified in the previous RAI.

R336.2. Comparisons of RPV heater power, RPV, DW and WW pressures and PCCS flows for PANDA Tests P1 and M3 and GIRAFFE/Helium Test H1 are shown in Figures 336.7 to 336.9. The PCCS flows were judged to be a more useful variable to compare than the water levels because the water levels do not change appreciably during these tests (see, e.g., the

plot of WW water levels for Tests M6/8 and P6 in Figure 336.5). Only in the case of the PANDA early-start tests (M9 and P2) and the tests with the DW initially filled with air (M7 and P3), for which there are no GIRAFFE counterparts, do the pool water levels change significantly.

The first comparison (Figure 336.7) shows the heater powers for the three tests after scaling adjustments. [[

]] Taken together, the comparison of the three tests, encompassing a wide range of scales, shows similar behavior of key response variables. Differences in the details of the responses can be explained. All three tests confirm the satisfactory performance of the PCCS for limiting the long-term containment pressure following a design-basis LOCA.

[[

Figure 336.1 Pressure Comparison for Tests M7 and P3

Figure 336.2 Wetwell Level Comparison for Tests M7 and P3

Figure 336.3 PCC Flow Comparison for Tests M7 and P3

Figure 336.4 Pressure Comparison for Tests M6/8 and P6

Figure 336.5 Wetwell Level Comparison for Tests M6/8 and P6

Figure 336.6 PCC and IC Flow Comparison for Tests M6/8 and P6

Figure 336.7 RPV Heater Power Comparison for Tests M3, H1 and P1

Figure 336.8 Pressure Comparison for Tests M3, H1 and P1

Figure 336.9 PCC Flow Comparison for Tests M3, H1 and P1

]]

References

1. "TRACG Qualification for SBWR", NEDC-32725P, August 2002.

2. "TRACG Qualification for ESBWR, NEDC-33080P, August 2002.

3. "ESBWR Test Report", NEDC-33081P, August 2002.

4. "GIRAFFE SBWR Helium Series Test Report", NEDC-32608P, June 1996.

Q337. Data from the passive containment cooling (PCC) vent phase detectors in the PANDA tests do not seem to be fully consistent with the DW and WW pressure data. For example, based on the pressure difference between the DW and WW for PANDA Test M3 shown on ALPHA-613-0/Page15 (M3 Data Transmittal Report), there was continuous PCC venting into WW. In contrast, data from PCC vent phase detectors (on ALPHA-613-0/Page 20) showed continuous PCC venting only at [[ ]] seconds and sporadic PCC venting afterwards. Please provide an explanation.

R337. During the long-term transient in Test M3 and in other similar PANDA tests, there is a pressure difference between the WW and DW, [[ ]] After the start-up of the PCCS and clearing of the initial DW air, there were no vacuum breaker openings in Test M3. The PCCS adjusted its heat removal capacity to meet the changing decay heat simulated in the RPV. After the initial air-clearing transient, flow to the PCCS was nearly all steam so, [[ ]] The pressure difference between the WW and DW was just equal to, or slightly below, the head required to clear the PCC vents so the PCCs [[ ]] as indicated by the vent phase detectors.

Q338. [[

]] Are there any PANDA data regarding the two-phase flow characteristics (e.g., void fraction, pressure drop) in the RPV chimney? Note that this question is in response to the Advisory Committee on Reactor Safeguards (ACRS) interest on the two-phase flow in the ESBWR partitioned chimney, which was reflected in the questions raised in the two recent ACRS meetings.

R338. The reviewer has correctly stated that the hydraulic diameter of the PANDA chimney is similar to that of the SBWR chimney partitions. There were no measurements of chimney pressure drop, so void fraction data are not available. As covered in RAI 179, the RPV in PANDA is primarily a steam generation source. The issue of chimney void fraction distribution is covered elsewhere; e.g. the Ontario Hydro test data (see TAPD Tables 5.1-1a. and 5.3-1a)

Q345. The DW water levels were measured in the PANDA tests but were not reported. Please provide this data?

R345. In both the PANDA M-series and P-series tests, DW levels were measured. These measurements were identified as instrument channels ML_D1 and ML_D2. Plots of these measurements for the M-series P-series tests are shown below as Figures 345.1 to 345.16. The water accumulation in the DW, even in the longest PANDA tests, [[ ]]
[[

Figure 345.1. Test P1/8 Drywell Levels

Figure 345.2. Test P2 Drywell Levels

Figure 345.3. Test P3 Drywell Levels

Figure 345.4. Test P4 Drywell Levels

Figure 345.5. Test P5 Drywell Levels

Figure 345.6. Test P6 Drywell Levels

Figure 345.7. Test P7 Drywell Levels

Figure 345.8 Test M2 Drywell Levels

Figure 345.9. Test M3 Drywell Levels

Figure 345.10. Test M3A Drywell Levels

Figure 345.11. Test M3B Drywell Levels

Figure 345.12. Test M6/8 Drywell Levels

Figure 345.13. Test M7 Drywell Levels

Figure 345.14. Test M9 Drywell Levels

Figure 345.15. Test M10A Drywell Levels

Figure 345.16. Test M10B Drywell Levels

]]

Q347. Page 2-3, 4th paragraph. [[

]] Please provide the basis for the decay heat load estimate at one hour after the scram.

R347. The RPV power for Test P3 was [[ ]] To force the system into an asymmetric mode, all of the RPV steam flow to DW1 was valved off and the PCC1 unit on DW1 was valved out. This was in contrast to the similar test (M7) in the M-series, which had all three PCC units in service. To compensate for the one PCC unit out of service, the P3 RPV power level was reduced to approximately two-thirds of the scaled one-hour decay power.

Q349. Pages 3-1 (last paragraph) and 3-3 (Fig. 3-1). It is stated that [[

]]

Q349.1. [[

]]

R349.1. [[

]]

Q349.2. [[

]]

R349.2. [[

]]

[[

Figure 349.1. RPV and GDCS Levels for PANDA Tests M9 and P2

]]

Q349.3. How many VB openings occurred in Test P2?

R349.3. There were two VB openings in Test P2. One occurred very close to the start of the test and a second occurred at about 7000s. The times of the VB openings are shown in Figure 21a of the P2 test report that was included in the Reference 3 submittal.

Q349.4. [[

]]

R349.4. [[

]]

Q349.5. Why was the peak DW pressure in Test P2 about 0.1 bar lower than in Tests P4 and P1/8?

R349.5. The lower DW pressure is associated with the lower WW pressure that results from the increase in the effective WW gas space as the GDCS pool drains to the RPV.

Q349.6. Why did the DW pressure decrease much faster at around 8000 seconds in Test P2 than in Tests P4 and P1/8?

R349.6 The flow of subcooled GDCS water to the RPV contributed to the DW pressure decrease in Test P2.

References

1. "TRACG Qualification for SBWR", NEDC-32725P, August 2002.

2. "TRACG Qualification for ESBWR, NEDC-33080P, August 2002.

3. "ESBWR Test Report", NEDC-33081P, August 2002.

4. "GIRAFFE SBWR Helium Series Test Report", NEDC-32608P, June 1996.

Q350. Page 3-4, Fig. 3-2.

Q350.1. Does each data point shown in Fig. 3-2 represent the WW pressure increase between the end of the test and the beginning of the test? In other words, ΔP_{nc} (of x-axis) = P_{nc} (at the end of the test in the WW) – P_{nc} (at t = 0 in the WW), and ΔP (of y-axis) = WW pressure (at the end of the test) – WW pressure (at t = 0).

R350.1. Yes, that is what is plotted.

Q350.2. Why did H1 and M3 fall below the 45-degree line? What is the physical implication?

R350.2. The results for Tests M3 and H1 show that the WW pressure increase was essentially equal to the increase in the noncondensable pressure. [[

]]

Q350.3. An improvement could be made to Fig. 3-2 by making the y-axis at the same length as the x-axis so that the 45-degree line would be truly the 45-degree line.

R350.3. The reviewer's suggestion has been incorporated in the replot of Figure 3-2, shown below as Figure 350.1.

[[

Figure 350.1 WW Pressure Increase vs. Increase in Noncondensable Partial Pressure

]]

Q351. ALPHA-716-0/Page 18 (Fig. 3 for Test P1/8).

Q351.1. Explain why the main steam line flow rate rose continuously between 0 and 900 seconds, as shown in Fig. 3. In other words, why didn't the peak flow rate occur at t = 0 seconds?

R351.1. The increase in steam flow rate during the first few minutes of Test P1/8 is the result of the heater bringing the RPV liquid to boil-off conditions. This also includes pressurization of the DW and start-up of the PCCS. This flow increase is part of the start-up transient for the test. Similar behavior can be observed in the other PANDA tests.

Q351.2. [[

]]

R351.2. [[

]]

Q352. ALPHA-716-0/Page 19 (Fig. 4). What was the reason for a drastic drop in the PCC1 feed flow rate at around 12,600 seconds (immediately after VB opening) as shown in Fig. 4?

R352. The drop in PCC flow is the result of the PCCS ingesting air following the vacuum breaker opening. As discussed in earlier responses, the flow to the PCC is driven by the pressure difference between the DW and the PCCS. When air enters the PCC, the pressure in the PCC increases because of the degradation of the condensation heat transfer. In response, the DW pressure increases and opens the PCC vents. The air is purged from the PCC tubes and the flow to the PCCs is restored.

Q353. ALPHA-716-0/Page 20 (Fig. 5). [[

]]

R353. [[

]]

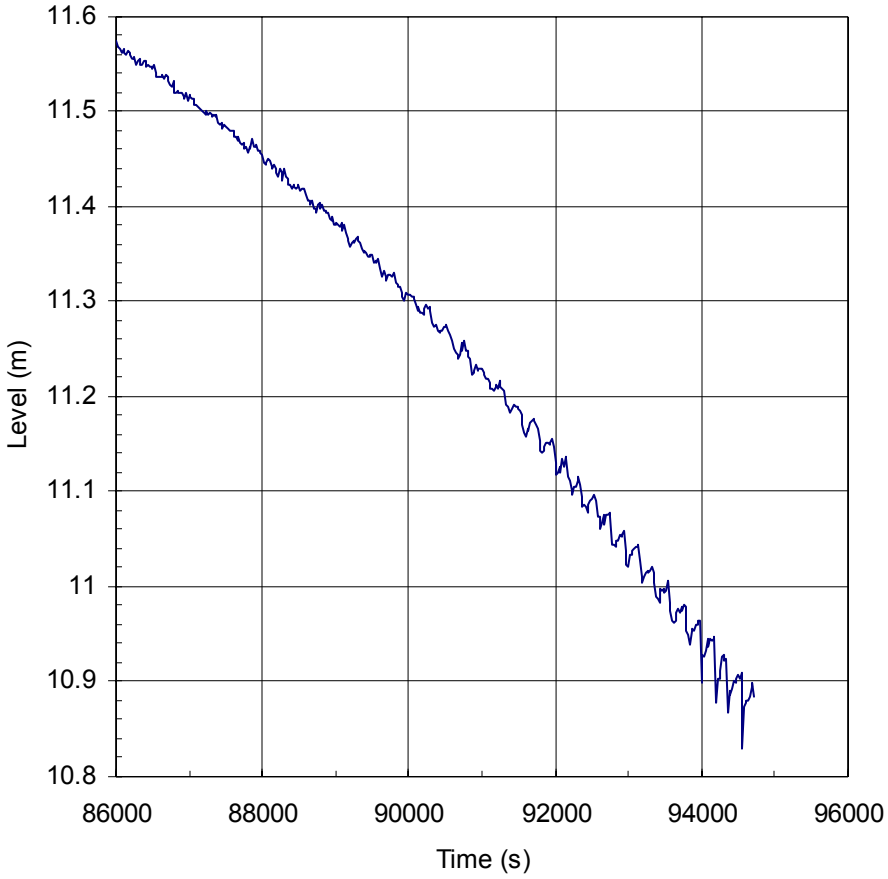

Figure 353.1. RPV Collapsed Level in Test P1/8

Q354. ALPHA-716-0/Page 24 (Fig. 9). As shown in Fig. 9 and stated on ALPHA-716-0/Page 14 (1st paragraph), the continuous temperature rise in the WW1 gas temperatures (MTG.S1.1 and MTG.S1.3) was due to DW steam condensation inside the main vent pipes (located inside the WW gas space) during the first 11 hours (39,600 seconds).

Q354.1. In contrast, what caused the gas temperature of MTG.S1.6 to decrease between 21,000 and 40,000 seconds?

R354.1. The measurement referred to in this question (MSTG.S1.6) was near the top of WW 1 and slightly removed from the location where the main vent entered the WW gas space. We have concluded that this instrument was outside the zone of influence of the main vent. After initial heat-up from pressurization and venting during the first 1000 seconds, the temperature in this region may have actually cooled slightly due to system heat losses. The decrease referred to in the question is much less than one degree so the effect is small.

Q354.2. What was the reason for the suppression pool surface temperature (MTS.S1.1) exceeding the gas temperatures (MTG.S1.6 and MTG.S1.3) for a large portion of the test duration?

R354.2. We believe the temperature differences referenced here were due to spatial temperature variations in the WW. The pool surface was hotter than the air space because [[

]] The pool surface temperature was also measured by a floating probe that measured three temperatures: one about 1 cm. below the surface; one at the surface; and a third about 1 cm. above the surface. The temperature reported was the surface temperature but, with few exceptions, these three temperatures were within a degree of each other. The air space temperatures higher up and away from the surface [[

]]

Q354.3. Explain why the VB opening at around 3.5 hours (12,600 seconds) was not reflected in the WW gas temperatures.

R354.3. When the vacuum breaker opened at 3.5 hours, air flowed out of the WW. If there were any response, it would have been a slight local cooling of the gas space. With some effort, one might attribute the very slight decrease in the temperature recorded by MTG.S1.6 at the time of vacuum breaker opening to this outflow. Any effect on the bulk temperature in the large WW airspace above the pool would be small.

Q355. ALPHA-716-0/Pages 26, 28, and 30. Comparing the PCC upper tube temperatures in PCC1 (Figs. 11a), PCC2 (Fig. 12a), and PCC3 (Fig. 13a), only the PCC1 tube gas temperature experienced a large decrease immediately after VB opening (at around 3.5 hours or 12,600 seconds). Does this decrease imply that at around 3.5 hours, the opening of VB1 occurred before the opening of VB2 so that DW1 received a larger portion of the noncondensible gas vented from the WW?

R355. This is a reasonable conclusion by the reviewer although it cannot be supported by direct experimental evidence. It is likely that the amount of air entering DW1 was similar to that entering DW2 but, with only one PCC on DW1, the effect on the PCC1 temperatures was greater than for the two PCC units connected to DW2.

Q356. ALPHA-716-0/Page 32. Why was the air partial pressure at mid-height of DW2 (MPG.D2.2) greater than that near the DW2 bottom (MPG.D2.3) as shown in Fig. 14?

R356. [[

]]

Q357. ALPHA-716-0/Page 33.

Q357.1. Why there was more air in WW2 (MPG.S2) than in WW1 (MPG.S1) by about 0.08 bar (1 psi)? Was this caused by the venting of two PCC units to WW2 (vs. the venting of only one PCC unit to WW1)?

R357.1. The greater air partial pressure in WW2 throughout the test was due to the test initial conditions (Table 6.1 of the test report). The initial difference persisted throughout the test but did not have a detrimental effect on the test results or on the accomplishment of the test objectives.

Q357.2. Why was the VB opening at around 3.5 hours (12,600 seconds) not reflected in the air partial pressure in the WW?

R357.2. Since the vacuum breaker flow was out of the WW airspace, there was no change in the ratio between the air and steam partial pressures. Any change would have to be due to a global air space pressure change resulting from the vacuum breaker opening. As can be seen from the plot of Figure 1 of the test report, the WW and DW pressures, the WW airspace is so large, that the vacuum breaker opening had a negligible effect on the WW pressure and therefore we would expect no change in the WW air partial pressure.

Q358. ALPHA-716-0/Pages 36 to 38. As shown in Fig. 18, all three PCC vent lines were not cleared between 20,000 and 40,000 seconds, while Fig. 5 (ALPHA-716-0/Page 20) shows continuous steam condensation in the PCC units. Does this imply that the PCC units are capable of condensing steam even when their vent lines are not cleared and are blocked with water?

R358. Yes, the PCCS is able to operate without venting. It is only necessary that the system maintain a sufficient length of condensing surface in the tubes to match the RPV heat load. The period cited was after the vacuum breaker opening when the DW had been cleared of air and the flow to the PCCs was nearly pure steam. There was a gradual buildup of noncondensable which led to vent clearing at about 50,000 seconds.

Q359. ALPHA-716-0/Pages 41 to 42.

Q359.1. Please provide an instrumentation diagram to show where these main vent thermocouples were located.

R359.1. The main vent instrument locations are shown in Figures 359.1 and 359.2. The thermocouples used to measure gas temperatures are identified as MTG.MV1.1 - 4 and MTG.MV2.1 - 4. Dimensions are in millimeters.

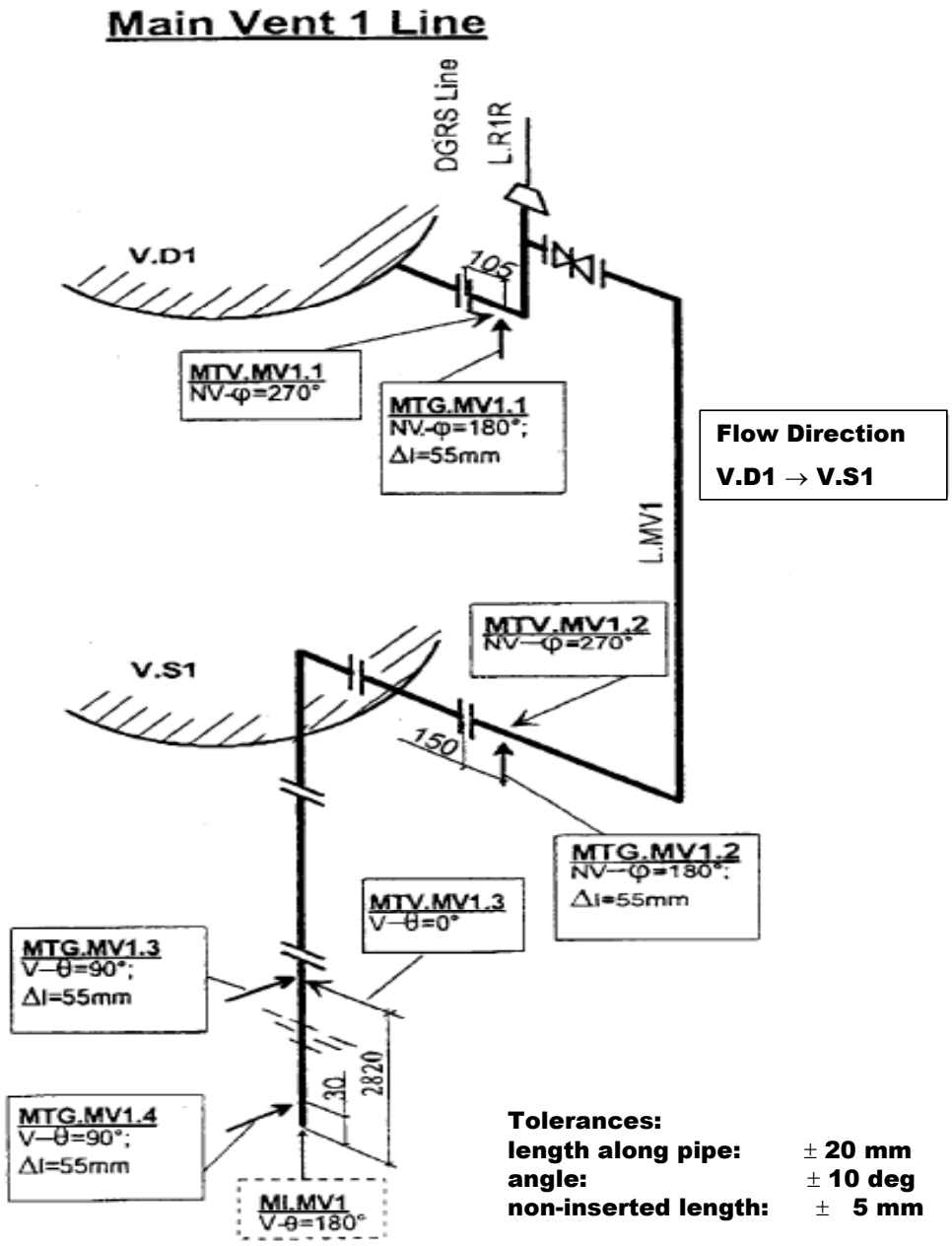

Figure 359.1. Main Vent 1 Instrument Locations

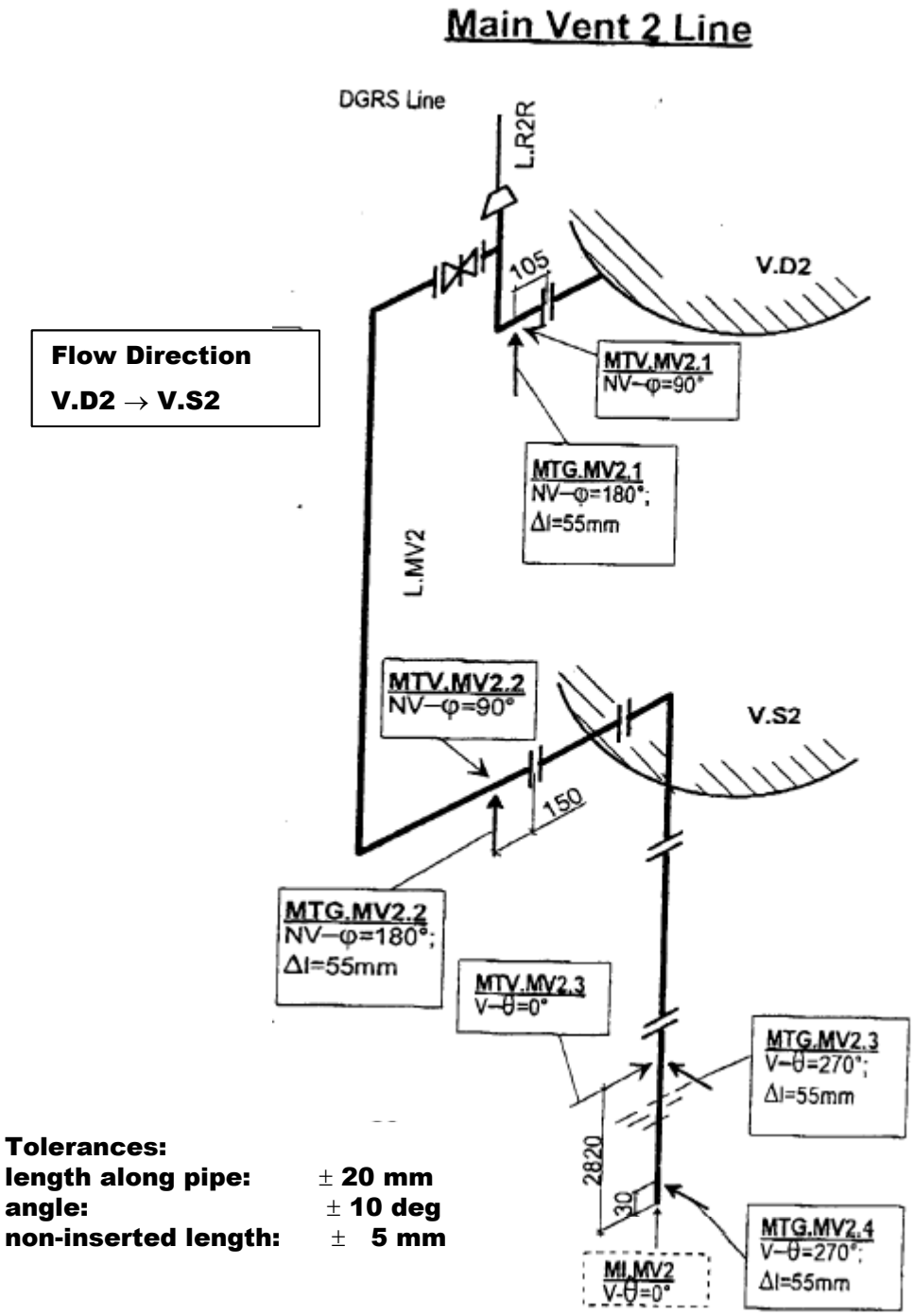

Figure 359.2. Main Vent 2 Instrument Locations

Q359.2. Explain why there was a rapid decrease in the temperatures of MTG.MV1.2 and MTG.MV1.3 at around 40,000 seconds.

R359.2. [[

]]

Q359.3. Explain why there was a temperature drop and recovery of MTG.MV1.3 at around 10,000 seconds.

R359.3. The temperature drop and recovery at 10,000 seconds is nearly coincident with the vacuum breaker opening. The main vent temperatures are responding to the DW pressure decrease prior to vacuum breaker opening and the subsequent pressure increase as flow to the PCCS decreases.

Q371. Page 2-54, 2nd paragraph. It appears incorrect to say that Test M2 is a repeat of Test M3, because all the break flow was directed into DW2 in Test M2.

R371. The reviewer's comment is accepted. The meaning of "repeat" in this context was that the initial conditions and RPV heater power vs. time were the same.

Q372. Page 2-54, last paragraph. Please quantify the bypass area that is ten times the scaled SBWR design value (in cm^2).

R372. Test M6/8 was conducted with a [[
]] The corresponding PANDA $A/\sqrt{K} = 0.4$ cm^2.

Q373. Page 2-61, last paragraph. Please explain the statement: "A design limitation of the test facility which does not permit two-phase flow from the RPV to the DW through the steam lines." Is this a concern to PANDA tests?

R373. Not permitting two-phase or liquid flow through the steam lines is not a concern for the PANDA tests. Only steam due to decay heat boil-off leaves the RPV during the long-term cooling phase of the ESBWR LOCA. As a practical matter, this requirement was placed on the PANDA facility to avoid damaging the low-flow measurement instrumentation in the steam line.

Q374. Page 2-67, 4th paragraph. Please add a figure to show the RPV, DW, and WW pressures and the PCC inlet mass flow rates (or add two separate figures if it is preferred). [[

]]

R374. [[

]]

Figures 336.1 and 336.2 (RAI336) show the RPV, DW and WW pressures and the PCC inlet flow rates for Test M7.

Q375. Page 2-68, 2nd paragraph. Please provide a comparison of air concentration (or partial air pressure) in the DW between Tests M3 and M9 to support the statement that more air remained in the DW in Test M9 than in Test M3.

R375. The reason for the pressure difference between Tests M3 and M9 is a slightly lower noncondensable inventory in Test M9. This was primarily associated with the fact that in Test M9 the initial GDCS pool level is about 3.3 m above the GDCS level in Test M3.

Q376. Page 2-75, Fig. 2.3-5.

Q376.1. In Fig. 2.3-5, how many times did VB open in PANDA Test M3A? It appears that there were only three VB openings based on the DW pressure drops shown in Fig. 2.3-5 (excluding the small pressure drop at 13,000 seconds), but the figure legend stated four VB openings in Test M3A.

R376.1. In Test M3A there were two periods where there were one or more vacuum breaker openings. These periods followed the last two of the four PCC pool refillings. The Figure 2.3-5 legend indicates the number of actual vacuum breaker openings that occurred in each of these periods. For Test M3A, there were four openings following the third refilling and one following the last refilling. Similarly, in Test M3B there were two openings following the last refilling. The multiple openings in each period were in quick succession and confined to the brief interval in which the DW pressure was depressed.

Q376.2. As stated on p. 2-63 (2nd paragraph), M3B showed decreases in the DW pressure when the PCC pools were refilled (Fig. 2.3-8). This statement appears to be true with one exception; Fig. 2.3-5 shows no DW pressure decrease for M3B at around 11,000 seconds when the PCC pools were refilled. What is the rationale for this exception?

R376.2. All of the DW pressure decreases in Figure 2.3-5 were the result of PCC pool refilling. Water was added to the PCC pool four times in Test M3B: at around 12,000s, 27,000s, 44,000s and 62,000s. Times are approximate because each pool refilling took place over a short time period. In the DW pressure plot (Figure 2.3-5), there are three distinct pressure decreases as the result of pool water additions and the corresponding enhancement of PCCS heat removal. The magnitude of the pressure decreases becomes larger with time as the PCC heat load decreases and a smaller fraction of the condenser tube length is required to condense the steam. This is evidenced by the fact that the first refilling did not produce a noticeable drop in the DW pressure and the last refilling was followed by a DW pressure decrease that resulted in two vacuum breaker openings.

Q378. Page 2-79, Fig. 2.3-9. Why was the DW pressure of Test M2 (asymmetric steam flow to the DW) lower than that of Test M3 in Fig. 2.3-9?

R378. In Test M2, all the steam flow was to DW2 and steam could only enter DW1 through the DW crossover pipe. Air in the DW1 region below the crossover pipe did not mix effectively with the incoming steam and remained stratified. This resulted in less air being transferred to the WW and, consequently, slightly lower WW and DW pressures in Test M2.

Q379. Page 2-80, Fig. 2.3-10. Since the DW pressure of Test 10A (2 PCC units) was either lower or the same as that of Test M3 (3 PCC units) as shown in Fig. 2.3-10, does this imply that 2 PCC units were sufficient to remove the decay heat for these PANDA tests?

R379. The fact that the DW pressures levels out at just [[ ]] for both Tests M3 and M10A does show that two PCC units are sufficient to remove the decay heat. The fact that the long-term pressures for the two tests are essentially the same is the result of two compensating effects. As stated in the response to RAI378, the asymmetric steam flow to DW2 allows stratification of noncondensable in DW1 and thereby lowers the pressure. The valving out of PCC1 for Test M10A [[

]] an amount that approximately balanced the effect of less noncondensable transfer so that the long-term pressures from the two tests were about the same.